Abstract for the 29th Intl Workshop on Water Waves and Floating Bodies, Osaka (Japan), March 30 – April 02, 2014

Comparisons of MPS and SPH methods: Forced Roll Test of a Two-dimensional Damaged Car Deck

by David Le Touzé*, Hirotada Hashimoto**, Nicolas Grenier*, and Makoto Sueyoshi***

* LHEEA Lab., Ecole Centrale Nantes / CNRS, Nantes, France
** Graduate School of Engineering, Osaka University, Osaka, Japan
*** Research Institute for Applied Mechanics, Kyushu University, Fukuoka, Japan
E-mail: *David.LeTouze@ec-nantes.fr*

Highlights:

- Systematic comparisons between the MPS and SPH methods as well as a model experiment are performed on forced roll tests of a two-dimensional damaged car deck, in terms of total hydrodynamic forces, local pressure and flood water deformations.
- In order to treat trapped air in damaged compartments, different approaches are proposed for each particle method.

1. Introduction

Collision and grounding accidents of ships are frequently reported even now. Securing the survivability under flooding condition is one of the most important subjects in ship design. For quantitative safety assessment of the damage ships, numerical simulation methods for dynamic behaviors of damaged ships are desired, which enable to simulate the ship motion from the beginning of water flooding to final equilibrium state. In order to predict fast and largely-deformed free surface flows related to flooding, e.g. down-flooding, sloshing and overturning, particle methods would be promising.

In this study, systematic comparisons between the MPS (Moving Particle Semi-implicit) and SPH (Smoothed Particle Hydrodynamics) methods, and a model experiment are performed on forced roll tests of a two-dimensional damaged car deck. Through the comparisons, capability of the particle methods for flooding problems and differences in prediction accuracy between the MPS and SPH methods are demonstrated. Finally we discuss how the trapped air in damaged compartments can be treated by the particle methods.

2. Particle Methods

2.1 MPS method

The MPS method was developed for solving incompressible fluid [1]. The MPS method is one of the meshfree particle methods, and can deal with violent free surface flows, e.g. sloshing, slamming and breaking waves. The governing equations of the MPS method, dealing with incompressible fluid, are expressed as Eq.1. The differential operators are calculated with discrete models called particle interaction models using a weight function. The gravity and the viscous terms are solved explicitly and the Poisson equation for the pressure is solved implicitly.

In this study, COMPS (COmputational code for Moving Particle Simulation) is used as the MPS solver. (See the details of the code [2]-[3]). The weight function used in this study is shown in Eq.2. In COMPS, ghost particles are not necessary to impose solid boundary condition by adopting the symmetry boundary (mirror symmetry) using normal vectors. Therefore, thin plate structures, e.g. car decks, shell plating and stiffeners of ships, can be treated with larger particle distance. Since the pressure at boundary particles is not solved in COMPS, weighted average pressure is calculated from neighbor particles with use of the weight function to estimate hydrodynamic forces acting on a body.

$$\frac{D\rho}{Dt}=0, \qquad \frac{D\boldsymbol{u}}{Dt}=-\frac{1}{\rho}\nabla p+\upsilon\nabla^2\boldsymbol{u}+\boldsymbol{g} \tag{1}$$

$$w(r)=\begin{cases}\left(\dfrac{r_e}{(r+r_e\times 0.05)}-1\right)-\left(\dfrac{r_e}{(r_e+r_e\times 0.05)}-1\right) & 0\le r<r_e\\ 0 & r_e\le r\end{cases} \tag{2}$$

2.2 SPH method

The SPH method derives from astrophysical field and was developed by Lucy [4] and Gingold & Monaghan [5]. The SPH governing equations deal with compressible fluids (cf. Eq.3) with a closure equation of state (Eq.4). Hyperbolic part of Eq.4-5 is solved through an approximate Riemann solver (called acoustic) with enhanced accuracy (MUSCL scheme). Second order differential operator in Eq.5 is calculated with standard SPH interpolator based on Wendland

kernel (Eq.5). Time forwarding is explicit for all equations.

In this study, SPH-Flow is used as the SPH solver (see the details [6]-[7]). Boundary conditions are enforced by the Normal Flux Method) which requires neither particles on the boundary nor ghost particles. This method reduces implementation complexity and allows to simulate more easily complex geometries. Special care is taken for the parallel implementation of the SPH scheme to keep an efficient scalability (almost perfect up to thousand of cores).

$$\frac{D\rho}{Dt}+\nabla(\rho \boldsymbol{u})=0, \qquad \frac{D\boldsymbol{u}}{Dt}=-\frac{1}{\rho}\nabla p+\upsilon\nabla^2\boldsymbol{u}+\boldsymbol{g} \tag{3}$$

$$p=f(\rho) \tag{4}$$

$$w(q)=\frac{7}{\pi}\begin{cases}(1-|q|)^4(4|q|+1) & |q|\le 1\\ 0 & |q|>1\end{cases} \tag{5}$$

3. Numerical Results

3.1 Model experiment

Forced roll tests were conducted at the 2-D basin of Osaka University. A simplified two-dimensional damaged car deck is selected as a subject. A schematic view of the model and its dimensions are shown in Fig.1 and Table 1. The model was made by acrylic and its thickness is 0.008m for the second car deck floor and the broadside opposite to the damage openings. A rotating moment is added by an electric servo motor with feedback control. The horizontal and vertical forces and the moment around the center of rotation were measured by a dynamometer. The height of rotation axis is 0.3m above from the model bottom. A pressure sensor with diameter of 1 cm is installed on the left-side inner wall, which coordinate is (-0.242, 0.160). A body-fixed coordinate system is used for analyses of the forced roll tests.

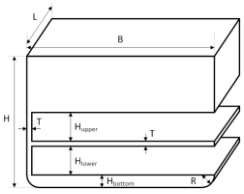

Fig. 1 Schematic view of the damage model.

Table 1 Dimensions of the damage model.

B	H	H_{bottom}	H_{lower}
0.5 m	0.35 m	0.035 m	0.085 m
H_{upper}	L	R	T
0.085 m	0.28 m	0.035 m	0.008 m

3.2 Numerical condition

The same numerical tank (see Fig.2) and the same distance of adjacent particles (0.0015m) are used in MPS and SPH simulations for the comparison purpose. Numerical conditions used for the MSP and SPH methods are shown in Tables 2-3, respectively. The total number of water particles is about 300,000. The forced roll test is realized by giving roll angular velocities to the boundary particles, consisting of the damaged body, with use of a sinusoidal function.

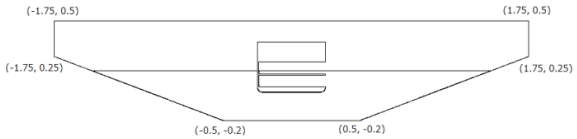

Fig.2 Numerical tank.

Table 2 Numerical condition (MPS).

Time step	Relaxation factor	Multiplication coeff.
0.0002 s (const.)	0.25 (ϕ_a=20deg) 0.3 (ϕ_a=30deg)	1.0025 (ϕ_a=20deg) 1.005 (ϕ_a=30deg)

Table 3 Numerical condition (SPH).

Courant number	Speed of sound	Ratio R/dx
0.375 (Runge- Kutta 4)	20 m/s	4

3.3 Results and discussion

Comparisons of hydrodynamic force and local pressure are shown in Figs.3-5. The comparison of free surface shape, for the 2 deck damage case with ϕ_a=20deg, T_ϕ=2.5sec, is shown in Fig.6. For the 1 deck damage case, the MPS and SPH methods agree with the model experiment quantitatively in F_y and M_x, while do qualitatively in F_z and pressure. For the 2 deck damage case with ϕ_a=20deg, the sharp drop/rise appears around t/T_ϕ=0.56 in F_y and M_x and successive oscillation occurs after them. A certain shift in the average value of F_z can be found particularly in the SPH. Although the similar trend can be found in the case with ϕ_a=30deg, the discrepancy becomes small in F_y and M_x. In any conditions, the MPS and SPH methods provide the quite similar results for F_y and M_x, and hence it is presumed that the major discrepancy comes from the entrapped air in the damaged compartment, which is neglected in both methods. The presence of the trapped air can be seen clearly in Fig.6.

4. Trapped Air Treatment

4. 1 MPS

In COMPS, the trapped air is treated with simple algorithm based on Boyle's law. Firstly relative height of the upper-right corner of the lower compartment to the water surface is evaluated. When the corner submerges into the water, the hydrostatic pressure at the average depth of the inside free surface is calculated as the initial value. From the next step, the pressure of compressed air is calculated by Boyle's law with the time-depending air volume and is given to free surface particles and non-wetted inner wall particles until the corner point emerges in the air again. Once the corner emerges, zero pressure is given to the free surface particles as usual manner. The compressed air treatment with Boyle's law does not increase the CPU cost because the pressure of compressed air can be easily given to the free surface particles as Dirichlet condition instead of zero pressure in solving the Poisson equation.

4. 2 SPH

With SPH-Flow, the approach to model trapped air is different: the choice is made to fully simulate the movement of this second phase. Thus an additional set of particles is required to discretize air domain (around 275k supplementary particles). These ones are evolved with the same SPH equations 4-5 as water particles but the closure equation of state 6 is adapted to reproduce compressibility of air. Special treatment to ensure mass conservation is also performed at the interface to be compatible with the use Riemann solver. Surface tension effects are not taken into account in the present case. To avoid excessive computational time, the speed of sound of air is artificially decreased to 50m/s. Real compressibility of air is no more respected but compared to actual convective velocities in the air, this condition ensure a weakly-compressibility assumption.

4. 3 Results and discussion

Numerical results of the MPS with Boyle's law and the two-phase SPH are compared in Figs.7-8. Here ϕ_a=20deg for 2 deck damage is selected, where the trapped air is most influential on F_y and M_x. The sharp drop/rise found in Fig.4 disappears in the SPH, while does not so in the MPS. The two-phase SPH agrees with the experimental result quantitatively in F_y, M_x and P. Although the prediction accuracy of the MPS with Boyle's law model is lower than the two-phase SPH, it would be acceptable for practical uses because the prediction accuracy, especially in M_x, is sufficiently improved as compared to the original model. There is still certain discrepancy in F_z between the experiment and the two calculations even taking account of the trapped air effects. This might be because smaller tank depth is used in the MPS/SPH simulations as compared to the model experiment, and reflected waves from the numerical beaches could interfere with the flooded water in the damaged compartments. Therefore, further investigation is expected with use of a larger numerical tank, which is equipped more efficient beaches in terms of wave absorption.

5. Conclusions

Systematic comparisons of model experiment and the MPS and SPH methods are performed on forced roll tests of a two-dimensional damaged car deck. As a result, it is demonstrated that MPS and SPH results are in good agreement with the model experiment when the trapped air effect is relatively small. However the agreement becomes worse when the trapped air exists. The two-phase SPH model provides quantitative accuracy even with the presence of trapped air, and the MPS model incorporating Boyle's law gives practical accuracy without increasing the computational cost.

Acknowledgement

This work was supported by Grant-in Aid for Scientific Research (No.25289317), and strategic young researcher overseas visits program for accelerating brain circulation of Japan Society for Promotion of Science.

References

[1] Koshizuka, S., Oka, Y., 1996, Moving particle semi-implicit method for fragmentation of incompressible fluid, Nuclear Science and Engineering, Vol. 123, pp. 421-434.

[2] Sueyoshi, M., Kashiwagi, M. and Naito, S., 2008, Numerical simulation of wave-induced nonlinear motions of a two-dimensional floating body by the moving particle semi-implicit method, Journal of Marine Science and Technology, Vol. 13, pp. 85-94.

[3] Sueyoshi, M., 2009, Numerical Simulation of Tank Sloshing with Thin Plate Structures by Using a Particle Method, Proceedings of the 19th International Offshore and Polar Engineering Conference, Vol.3, pp.303-307.

[4] Lucy, L.B., 1977, A numerical approach to the testing of the fission hypothesis, Astron. J., vol. 82, pp. 1013-24.

[5] Gingold, R.A., Monaghan, J.J., 1977, Smoothed particle hydrodynamics : theory and application to non-spherical stars. Monthly Notices of the Royal Astronomical Society, 181, pp. 375-389.

[6] Le Touzé, D., Marsh, A., Oger, G., Guilcher, P.-M., Khaddaj-Mallat, C., Alessandrini, B., Ferrant, P., 2010, SPH simulation of green water and ship flooding scenarios, J. Hydrodynamics 22, supplement: 231-236.

[7] Maruzewski et al., Oger, G., Doring, M., Alessandrini, B., Ferrant, P., 2010, J. Hydraul. Res. 48, Extra Issue, pp. 126-134.

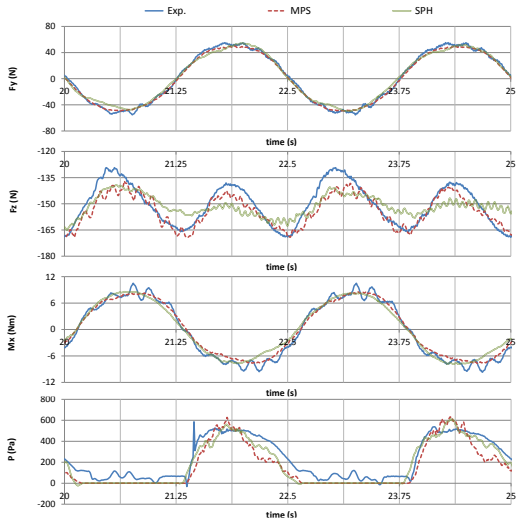

Fig.3 Comparison of the hydrodynamic force for 1 deck damage with ϕ_a=20deg, T_ϕ=2.5sec.

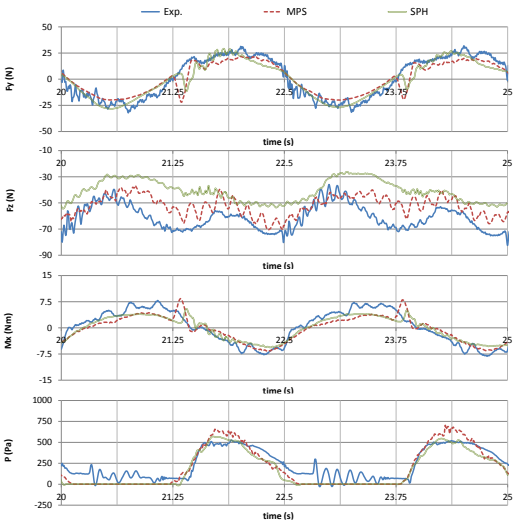

Fig.4 Comparison of the hydrodynamic force for 2 deck damage with ϕ_a=20deg, T_ϕ=2.5sec.

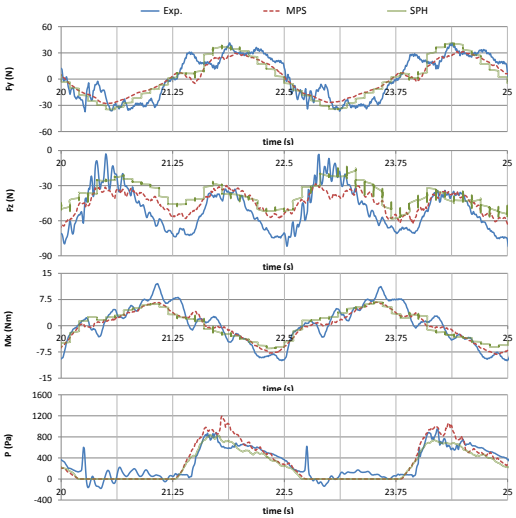

Fig.5 Comparison of the hydrodynamic force for 2 deck damage with ϕ_a=30deg, T_ϕ=2.5sec.

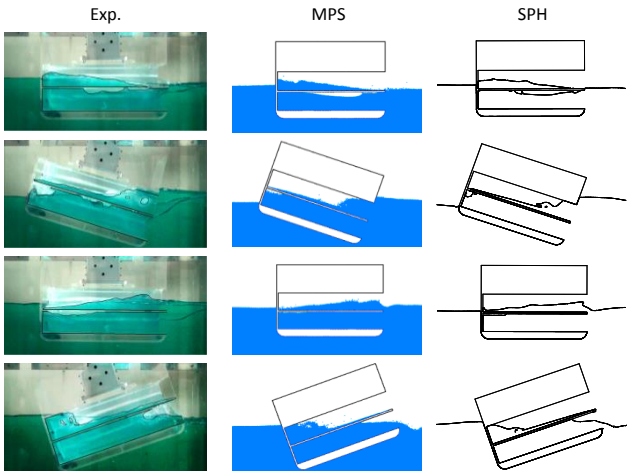

Fig.6 Comparison of the free surface for 2 deck damage with ϕ_a=20deg, T_ϕ=2.5sec (t=22.5, 23.0, 23.75, 24.25 sec).

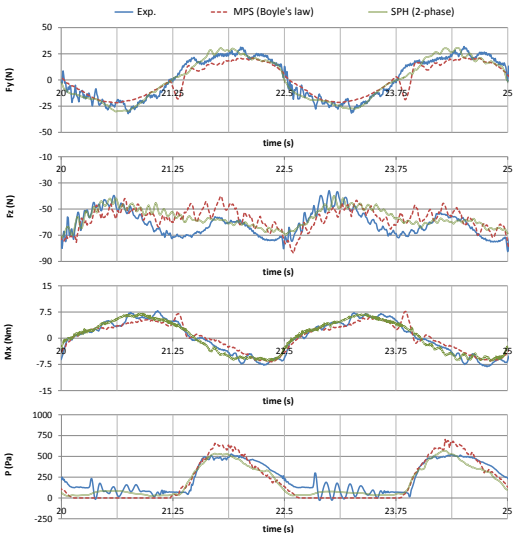

Fig.7 Comparison of hydrodynamic force for 2 deck damage with ϕ_a=20deg, T_ϕ=2.5sec.

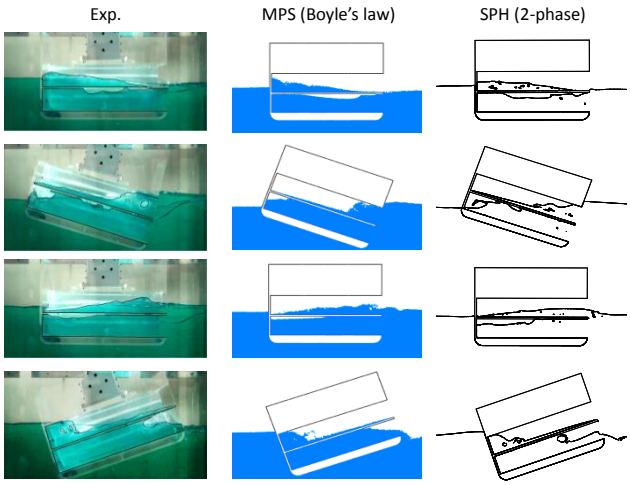

Fig.8 Comparison of the free surface for 2 deck damage with ϕ_a=20deg, T_ϕ=2.5sec (t=22.5, 23.0, 23.75, 24.25 sec).